Available online at www.sciencedirect.com

ScienceDirect

Underground Space 4 (2019) 251–260

www.elsevier.com/locate/undsp

Deformation behavior and acting earth pressure of three-hinge precast arch culvert in construction process

Yasuo Sawamura [a,*], Hiroyuki Ishihara [b], Yoshinori Otani [c], Kiyoshi Kishida [d] Makoto Kimura [a]

[a] Department of Civil and Earth Resources Engineering, Kyoto University, Japan
[b] Hokkaido Branch, Kajima Corporation, Japan
[c] Hirose Hokyodo & Co., Ltd., Japan
[d] Department of Urban Management, Kyoto University, Japan

Received 19 February 2018; received in revised form 27 September 2018; accepted 27 September 2018
Available online 2 November 2018

Abstract

The three-hinge precast arch culvert consists of two segmental precast units and three hinge points. It harnesses the passive resistance of an embankment by permitting deflection, resulting in a mechanically stable structure. However, the design of the three-hinge precast arch culvert differs from that of a conventional culvert, prompting the mechanical behavior of the culvert to become an important issue. In this study, therefore, 1/5 scale model tests were conducted on a three-hinge precast arch culvert to measure the changes in the inside width and earth pressure acting on the culvert at each step in order to investigate the culvert's mechanical behavior at each construction stage. Moreover, the deflection measurement of the culvert was obtained at the in-situ construction site. The results indicate that the arch members were displaced according to the embankment depth in a similar manner to the design load. Therefore, the horizontal earth pressure, which was larger than the earth pressure at rest, acted on the culvert at the end of its construction.

Keywords: Precast arch culvert; Construction process; Coefficient of earth pressure; Inside width

1 Introduction

The decline in the working population is becoming a serious problem in Japan, and improving productivity at construction sites is a pressing issue. Therefore, in culvert construction, the use of hinged precast arch culverts with precast components has attracted attention as a countermeasure. The advantages of hinged precast arch culverts are the high quality control and labor-saving assembly that can be obtained by using precast products. Two types of hinged precast arch culverts are used: the two-hinge precast arch culvert, which has hinges at both shoulders, and the three-hinge precast arch culvert, which has hinges at both the feet and the crown. Although these culverts have hinge functions at different positions based on the different design concepts, they are both constructed with thin members that allow for motion and rotation to mobilize earth pressure, as opposed to a rigid culvert that supports external forces using the rigidity of its members.

The three-hinge precast arch culvert, which is the object of this study, consists of two arch members and three hinges in the body. Figure 1 illustrates the structure of a typical three-hinge precast arch culvert. The culvert shape is determined in such a manner as to minimize the tensile forces in the arch members, creating an axially loaded structure (Hutchinson, 2004). The hinge points are located at the crown and both feet of the arch. Although a crown

* Corresponding author.
E-mail address: sawamura.yasuo.6c@kyoto-u.ac.jp (Y. Sawamura).

https://doi.org/10.1016/j.undsp.2018.09.005

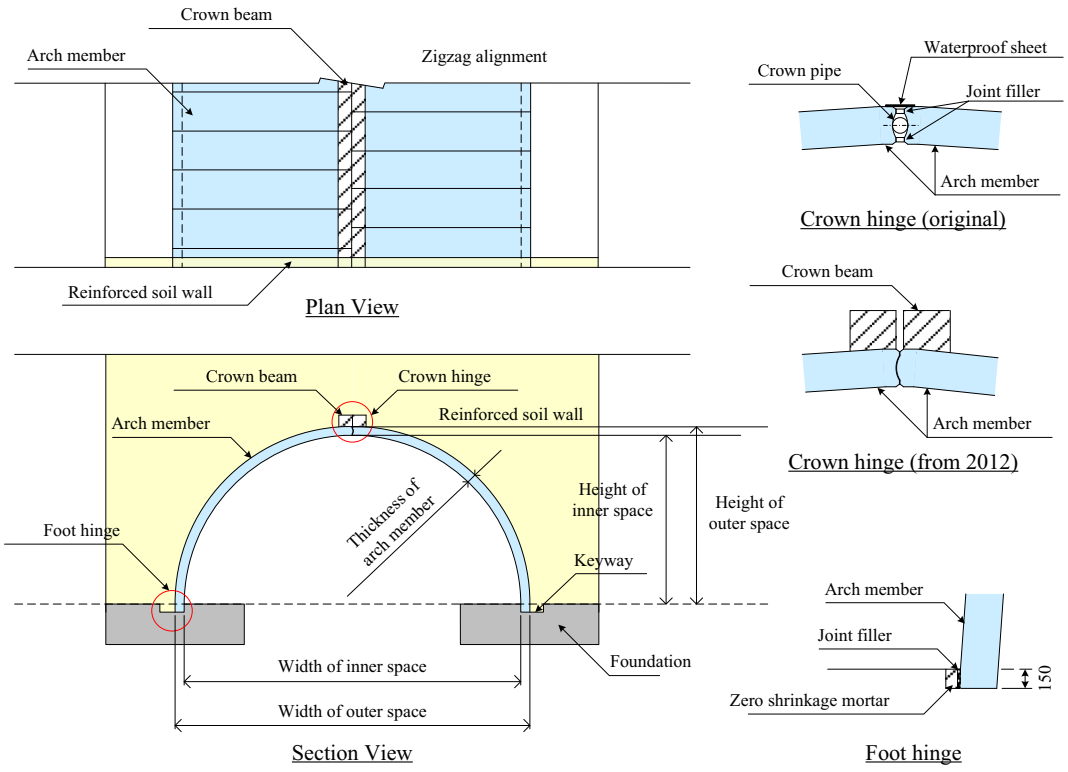

Fig. 1. Three-hinge precast arch culvert.

pipe and grout were used in older culverts to form the crown hinge, the two arch members lean against one another in current designs to form the crown hinge, and the crown beam is cast in-situ to support the arches against longitudinal loads. Moreover, at the foot hinges, each arch member is supported by independent concrete strip foundations or a single concrete slab. The foundation size is dependent on the soil conditions, structure size, and depth of the backfill above the arch. The arch members are placed in slots using a rubber joint filler, with a thickness of approximately 5 mm, which provides the hinge function at both feet. The arch width is within the range of approximately 5 to 20 m, while the arch height is within the range of approximately 30% to 70% of the width.

Regarding box culverts or rectangular underground structures, research on the behavior of culverts during construction (for example, Kim and Yoo, 2005; Pimentel, Costa, Felix, & Figueiras, 2009; Abuhajar, El Naggar, & Newson, 2015), while in service (for example, Acharya, Han, & Parsons, 2016; Wood, T. A., Lawson, W. D., Surles, J. G., Jayawickrama, P. W., & Seo, 2016; Abuhajar, El Naggar, & Newson, 2016), and during earthquakes (for example, Wang 1993; Debiasi, Gajo, & Zonta, 2013; Hushmand et al., 2016) is available. Focusing on the studies of culvert behavior during the construction stage, Kim and Yoo (2005) conducted linear and nonlinear finite element analyses to investigate the effective density or soil-structure interaction factor for deeply buried concrete box culverts. Based on the results, it was concluded that the soil-structure interaction factor for deeply buried box culverts depends on the foundation characteristics. Pimentel et al. (2009) carried out numerical and experimental studies on reinforced concrete box culverts with high embankment depths, and suggested that the soil pressure and culvert nonlinear behavior are directly related and should be considered in the design stage to achieve a more rational and economical design. Abuhajar et al. (2015) investigated the soil-culvert interaction, considering the height and density of the soil above the culvert and the culvert geometry. From their results, it was concluded that the soil-culvert interaction factor is not only a function of the height of the soil column above the culvert, but also of the culvert thickness, soil elastic modulus, and Poisson's ratio.

However, for hinged precast arch culverts, although the culverts have hinge functions and the design concept is completely different from that of conventional box culverts, few model tests on culverts during the construction process (Adachi, Kimura, Kishida, & Samejima, 2001a; 2001b) or numerical seismic analyses (Byrne, P. M., Anderson, D. L., & Jitno, 1996; Wood and Jenkins, 2000; Sawamura, Kishida, & Kimura, 2015) have been conducted. Adachi et al. (2001a; 2001b) performed model tests using acrylic plates and aluminum rods for the model lining and ground, respectively. They measured the vertical force acting on the linings and ground bottom, as well as the bending moment induced in the lining. Moreover, they investigated a method for reducing the load acting on the tunnel using soft material above the culvert. However, their

culvert modeling was limited, and precise deformation and earth pressure distribution were not observed. Byrne et al. (1996) conducted static, pseudodynamic, and dynamic finite element analyses for an embankment including a three-hinge arch culvert. The results indicated that the axial force acting on the culvert is significantly affected by the vertical acceleration, while the bending moment is significantly affected by the horizontal acceleration. Wood and Jenkins (2000) concluded that the bending moment distribution in the arch from horizontal dynamic loading is highly sensitive to the backfill and surrounding soil stiffness properties, and rather less sensitive to those of the foundation soils beneath the arch. From these studies, it was confirmed that the culverts exhibit satisfactory earthquake resistance. However, the aim of past studies was to comprehend the fundamental vibration characteristics and identify the stress concentration points. Thus, the effects of the changes in the structural strength of the concrete and the reinforcing bars after yielding, as well as the critical state as a whole, have not been investigated. Furthermore, because several conventional three-hinge arch culverts, which have a crown pipe at the crown hinge and were constructed as highway embankments, suffered damage in the 2011 Tohoku Earthquake, it is vital to elucidate the critical state of these culverts and their behavior during strong earthquakes.

Under these circumstances, the authors conducted 1/5 scale shaking table tests on a three-hinge precast arch culvert to clarify the seismic behavior and damage morphology of the culvert during excitation in the culvert transverse direction, using a strong earthquake response simulator (Sawamura, Ishihara, Kishida, & Kimura, 2016). In the tests, the changes in the inside width and earth pressure acting on the culvert were also measured at each step in the model ground preparation to investigate the culvert mechanical behavior at each construction stage. Moreover, deflection measurement of the culvert was obtained at the in-situ construction site. This paper describes the results of the culvert behavior across the construction stages by means of model experiments and field measurements.

2 Design concept of three-hinge precast arch culvert

A hinged precast arch culvert is a flexible structure that allows for the deformation of its members by means of hinge functions provided on the main body cross-section. Therefore, the culvert is stabilized by actively using the reaction force of the surrounding backfill. In this case, a design method for three-hinge precast arch culverts is described with reference to conventional rigid box culverts.

Figure 2 provides an illustration of the design load acting on a box culvert in the Japanese design. In the design of box culverts, the vertical earth pressure p_{vd} and horizontal earth pressure p_{hd} are considered using the following equations:

$$p_{vd} = \alpha \cdot \gamma \cdot h\left(\mathrm{kN/m^2}\right), \tag{1}$$

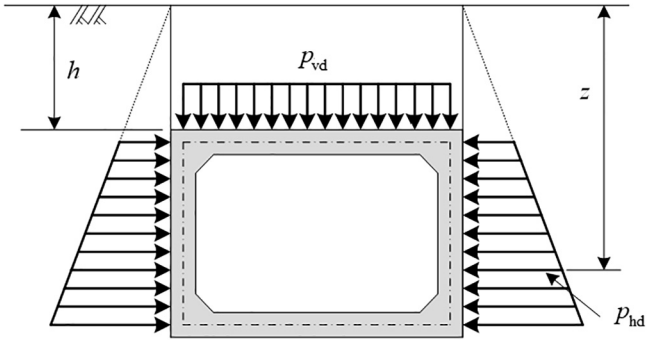

Fig. 2. Illustration of load acting on box culvert in Japanese design.

$$p_{hd} = K_0 \cdot \gamma \cdot z(\mathrm{kN/m^2}), \tag{2}$$

where α is the coefficient of vertical earth pressure, γ is the unit weight, kN/m^2, h is the overburden, m, K_0 is the coefficient of earth pressure at rest (usually $K_0 = 0.5$), and z is the depth, m. As the vertical earth pressure on a rigid culvert is greater than the weight of the soil above the structure (see, for example, Penman, Charles, Nash, & Humphreys, 1975; Vaslestad, Johansen, T. H., & Holm, 1993), the coefficient of vertical earth pressure α increases as the embankment height increases. Although both the magnitude and distribution of the earth pressure on a buried culvert are known to depend on the relative stiffness of the culvert and soil, the deformation of the members is not considered in the box culvert design.

However, the three-hinge precast culvert design differs from that of the box culvert. Figure 3 illustrates the deformation mode presumed in the design of a three-hinge precast arch culvert. In the current design, it is believed that when the embankment surface is lower than the culvert crown, the crown is displaced upwards because the horizontal earth pressure dominates. However, when the ground surface is higher than the crown, the overburden dominates, and it is believed that the crown is gradually depressed downwards and the arch flattens. Therefore, it is presumed that the horizontal earth pressure acting on the culvert is larger than the earth pressure at rest. This behavior has been qualitatively confirmed by means of model experiments (Adachi et al. 2001a; 2001b) and FEM analyses (for example, Segrestin and Brockbank, 1995). In this paper, the results of the field measurements and model experiments are presented based on this design presumption.

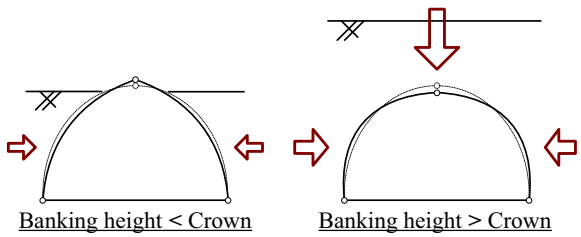

Fig. 3. Deformation mode of three-hinge precast arch culvert presumed in design.

3 Field measurements

3.1 Construction conditions

Figure 4 illustrates the field situation of the constructed three-hinge precast arch culvert. A cast-in-place arch culvert was originally planned for construction at this site, but a three-hinge precast arch culvert was constructed instead owing to the shorter construction period. The construction period was reduced by approximately 80%.

Figure 5 and Table 1 present a schematic drawing and the conditions of the in-situ construction, respectively. The arch culvert was 6.3 m high and 9.5 m wide. The coefficient of subgrade reaction of the foundation ground was investigated by means of plate bearing tests. Table 2 displays the material properties of the foundation ground. It was made of sandstone, and therefore, exhibited sufficient strength as a bearing layer. The maximum overburden soil above the arch culvert was 13.8 m. The field measurements were carried out from the beginning of May to the end of February of the following year (10 months). The changes in the inside width and earth pressure in the surrounding soil during the construction were measured at the measurement points indicated in Fig. 5.

Fig. 4. Field situation of constructed three-hinge precast arch culvert.

3.2 Measurement results

Figure 6 illustrates the change in the inside width during construction. The inside width changed when the embankment depth exceeded the crown height (6.3 m). When the embankment height was lower than the culvert crown, the crown was displaced upwards and the inside width decreased. However, when the embankment height exceeded the crown height, the crown was displaced downwards and the inside width increased. This behavior is almost the same as that assumed in the design. Regarding the change in culvert width, a large deformation occurred at $2h/4$ and $h/4$, and it was approximately 13 mm wider than the initial section. Moreover, the changes at these positions were 25 mm more than when the height of embankment was 6.3 m and the culvert width was the narrowest. Furthermore, even at the position of $3h/4$, although the deformation after construction did not differ significantly from the initial section width, it changed by approximately 18 mm from the narrowest value (embankment height: 6.3 m).

Figure 7 illustrates the change in the coefficient of earth pressure during construction. An earth pressure gauge was placed at a location 1 m from the culvert surface. Both the vertical and horizontal earth pressures were measured at each measurement point. The coefficient of earth pressure is defined as the horizontal earth pressure divided by the vertical earth pressure. The coefficients of earth pressure at the upper point (P-1) and lower point (P-2) were approximately 0.69 and 0.5, respectively. The coefficient of earth pressure at P-1 was larger than that at P-2 is owing to the culvert deformation. As the arch was compressed and flattened, it is believed that a greater lateral earth pressure acted on the shoulder parts of the arches.

Based on these results, it is confirmed that the deformation mode of the three-hinge arch culvert during the construction stage is consistent with the design assumption.

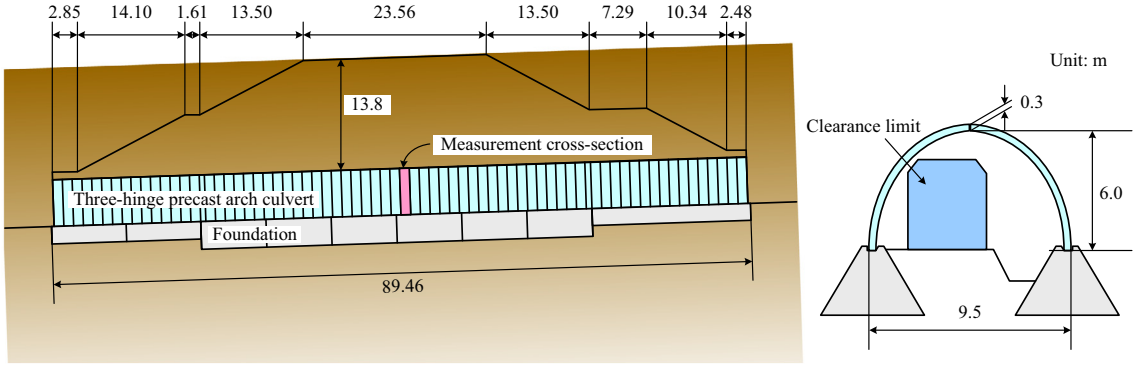

Fig. 5. Schematic of in-situ construction and measurement cross-section.

Table 1
Conditions of situ construction.

Item	Structure/Shape
Inside width (m)	9.5
Inside height (m)	6.0
Thickness of arch member (m)	0.3
Maximum overburden (m)	13.80
Transverse slope (%)	3.33
Construction extension (m)	89.46
Foundation	Unreinforced concrete

Table 2
Material properties of foundation ground.

Ultimate bearing capacity Q (kPa)	3.12×10^4
Coefficient of subgrade reaction K_s (kN/m^3)	3.24×10^5
Coefficient of subgrade reaction K_r (kN/m^3)	7.71×10^5
Deformation modulus E_0 (kN/m^3)	1.66×10^7
Internal friction angleϕ (°)	40.0
Cohesion c (kPa)	323.4

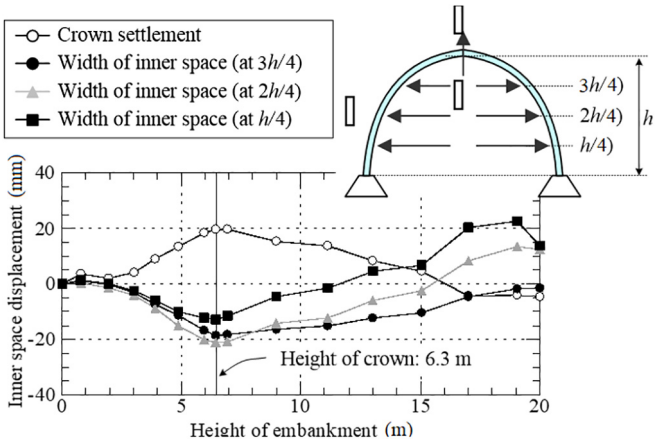

Fig. 6. Change in inside width during construction.

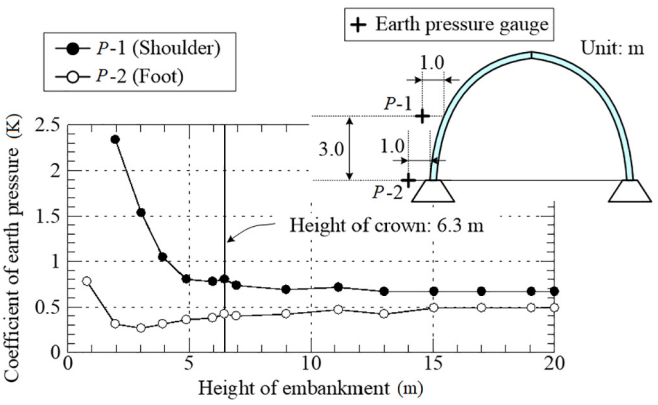

Fig. 7. Coefficient of earth pressure during construction.

4 Model experiments

4.1 Experimental outline

In this study, large-scale shaking table tests were conducted using the Strong Earthquake Response Simulator (SERS) at the Disaster Prevention Research Institute (DPRI), Kyoto University. Table 3 displays the apparatus specifications. The shaking table side was 5 m wide and 3 m deep. The SERS consisted of a 3D, six degrees-of-freedom shaking table that could move horizontally in two directions (X-axis and Y-axis), vertically (Z-axis), and rotate around the three axes (θ_x, θ_y, and θ_z) simultaneously or independently. In this paper, the mechanical behavior of the three-hinge precast arch culvert during the construction process is discussed. The dynamic behavior was reported in a previous paper (Sawamura et al., 2016).

A soil chamber, approximately 3.5 m long, 2.0 m deep, and 1.0 m wide, was used for the tests. The soil chamber had a window in the front wall, because it was necessary to install measurement instruments in the inner cavity of the culvert model and confirm the damage to the culvert following each excitation. The soil chamber permitted simple shear deformation as the lower part of the side wall and bottom of the soil chamber were connected by a hinge. Teflon and rubber sheets were attached to the soil chamber surface to reduce the friction between the soil and soil chamber.

Figure 8 illustrates the culvert model set-up and arrangement of the sensors. The changes in the inside dimensions of the culvert and wall displacement of the soil chamber were measured by laser displacement sensors (LB-300, produced by KEYENCE Corporation). Contact displacement gauges (CDP-25M, produced by Tokyo Sokki Kenkyujo Co., Ltd.) were used to measure the rotation angle and slippage of the crown hinge. The earth pressure acting on the culvert was measured by earth pressure

Table 3
Specifications of SERS.

Shaking direction	Horizontal (X, Y), Vertical (Z), Rotation (θ_x, θ_y, θ_z)
Maximum load	Rated: 15 000 kg, Maximum: 30 000 kg
Maximum displacement	Horizontal (X): ±300 mm Horizontal (Y): ±250 mm Vertical (Z): ±200 mm
Maximum velocity	Horizontal (X): ±1.5 m/s Horizontal (Y): ±1.5 m/s Vertical (Z): ±1.5 m/s
Maximum acceleration (Load 15 000 kg)	Horizontal (X): ±1 m/s^2 (±1.5 m/s^2 without load) Horizontal (Y): ±1 m/s^2 (±1.5 m/s^2 without load) Vertical (Z): ±1 m/s^2 (±1.5 m/s^2 without load)
Maximum rotation angle	X-, Y-, Z-axis (θ_x, θ_y, θ_z): ±3°
Frequency	DC ~ 50 Hz
Input wave	Sine, Random, Arbitrary

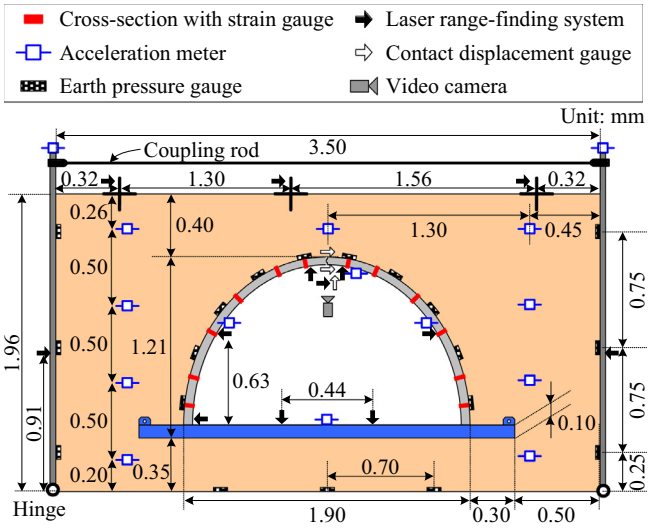

Fig. 8. Set-up of three-hinge culvert model and arrangement of sensors.

gauges (KDC-200KPA, produced by Tokyo Sokki Kenkyujo Co., Ltd.). The diameter, capacity, and degradative ability of the earth pressure gauges were 100 mm, 200 kPa, and 0.1 kPa, respectively.

The culvert model was constructed from reinforced concrete. Table 4 displays the material parameters of the culvert model. Kagawa (1978) described the similarity rule for the model tests in the 1G gravitational field. If the similarity rule is applied, it is necessary to reduce the culvert elastic modulus according to the model scale. However, it is difficult to control the concrete elastic modulus, and plastic behavior cannot be satisfied. Therefore, in this experiment, the material parameters of the concrete and reinforcing bars were not reduced for the 1/5 scale model culvert. When the member thickness was determined, a real culvert of 9.0 m width and 6.3 m height was firstly designed, following which the culvert scale was reduced to 1/5. Table 5 displays various physical properties when the similarity rule by Kagawa (1978) is applied. It is necessary to reduce the elastic modulus to 0.447 times its original value when using a 1/5 scale experimental model. Therefore, the culvert model used in this study has a relatively higher stiffness than an actual culvert. The dimensions of

Table 4
Design conditions and material properties of culvert models.

Design conditions and material properties		Three-hinge precast arch culvert	
		Design	1/5 model
Size	Inside height (m)	5.30	1.06
	Inside width (m)	9.00	1.60
	Overburden (m)	2.00	0.40
Concrete	Compressive strength f_c (N/mm^2)	35.0	47.4
	Young's modulus E_c (N/mm^2)	29.5	32.4
	Poisson's ratio ν_c	0.20	0.18
Reinforcing bar	Yield strength f_y (N/mm^2)	490.0	547.5
	Young's modulus E_s (N/mm^2)	200.0	190.2

Table 5
Similarity rule for model tests in 1G gravitational field, as proposed by Kagawa (1978).

Parameter	Similarity rule in 1G (Model /Practice)	
	Scale: 1/λ	Scale: 1/5
Length	1/λ	1/5
Frequency	$\lambda^{3/4}$	3.34
Density	1	1
Displacement	1/$\lambda^{3/2}$	0.089
Strain	1/$\lambda^{1/2}$	0.447
Elastic coefficient	1/$\lambda^{1/2}$	0.447
Stress	1/λ	1/5
Acceleration	1	1

the design culverts and 1/5 scale models are listed in Table 4.

Figure 9 presents a drawing of the culvert model rebar arrangement. The number of reinforcing bars was determined so that the reinforcement ratio (cross-sectional area of reinforcing bars to total cross-sectional area) would be close to that of a real structure. The three-hinged model was constructed using 5-mm bars for reinforcement so that the number of reinforcing bars would not be excessively small. Figure 10 illustrates the hinge structure of the experimental model. In this experiment, as indicated in Fig. 10 (a), the joint at the top expresses the hinge function as a butt structure consisting of matching concave and convex members, as in an actual structure. When assembling the arch members, the left and right members (four pieces on each side) were placed in a staggered arrangement, as in an actual structure. Sponge tape was placed between the culvert model and soil chamber to prevent the soil from falling through. Two foundation types exist for culverts: the footing type, in which an independent foundation is provided for each foot, and the invert type, in which the foundations of both feet are integrated into one founda-

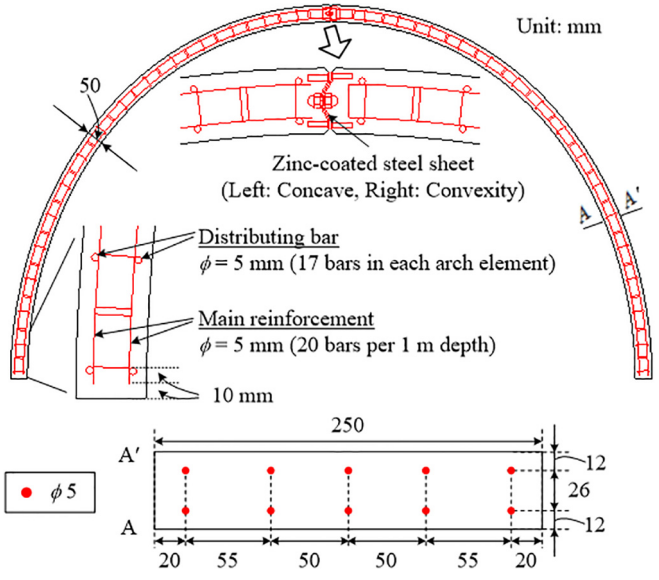

Fig. 9. Rebar arrangement of culvert model.

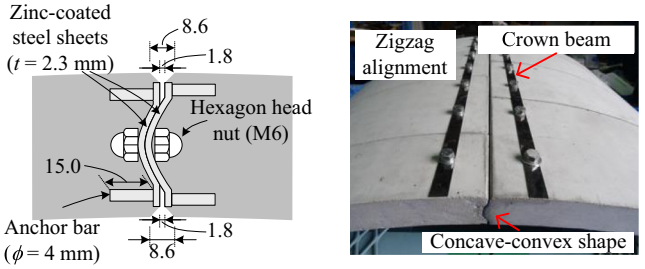

(a) Crown hinge

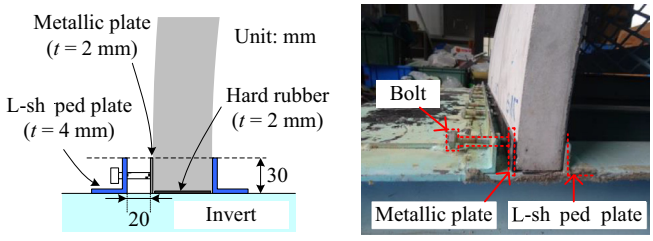

(b) Foot hinge

Fig. 10. Hinge structure of experimental model.

tion. In both types, the foundation is constructed so that no displacement occurs at the feet. In this experiment, because the foundation size that could be reproduced in the soil chamber was restricted by the soil chamber volume, the invert foundation was used, which suppresses the deformation of the feet (Fig. 11). To prevent deformation of the invert, H beams (100 mm × 100 mm) and steel plates (SS 400) were used to provide sufficient strength. A protective basket, made of H beams, steel plates, and expanded metals, was also attached to the invert to facilitate the measurement of the culvert relative displacement and protect the measuring instruments. At the foot hinges in actual construction, rubber joint material with a thickness of approximately 5 mm and non-shrink mortar are placed in the foundation grooves. Although this rubber joint material allows for hinge rotation at the feet, the rotation performance of the foot hinges is unclear. Therefore, in this experiment, the foot hinges were modeled as the simple structure illustrated in Fig. 10(b). The arch feet were set on a hard rubber sheet with a thickness of 2 mm, and the feet were sandwiched with bolts between two plates (an L-shaped plate from the inside and a metallic plate from the outside).

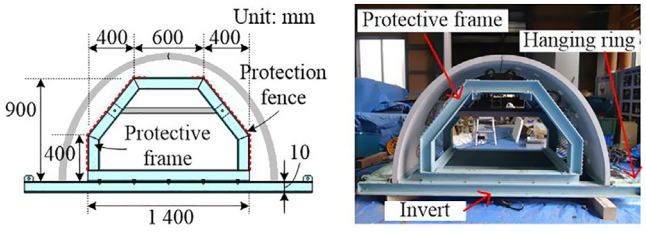

Fig. 11. Foundation of culvert and protective basket facilitating measurement.

Both the foundation ground and filling were made from Edosaki sand. The material properties, grain-size distribution curve, and compaction curve of the Edosaki sand are provided in Table 6, Fig. 12, and Fig. 13, respectively. Prior to preparing the model ground, the Edosaki sand was mixed with water to obtain the prescribed water content ($w = 20.0\%$). Thereafter, the model ground was prepared in 39 layers, one every 50 mm, by means of the compacting method. The compaction degree for the Edosaki sand was

Table 6
Material properties of Edosaki sand.

Gravel fraction (%)	0.6
Sand fraction (%)	89.8
Silt fraction (%)	3.7
Clay fraction (%)	5.9
Maximum grain size D_{max} (mm)	4.75
Average grain size D_{50} (mm)	0.19
Specific gravity of soil particle G_s	2.73
Optimum water content w_{opt} (%)	20.8
Maximum dry density ρ_{dmax} (g/cm^2)	1.64
Internal friction angle ϕ (°)	38.3
Cohesion c (kPa)	14.0

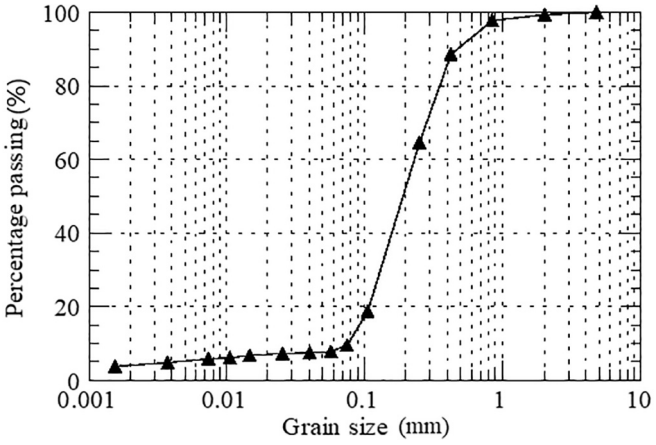

Fig. 12. Cumulative grain-size distribution of Edosaki sand.

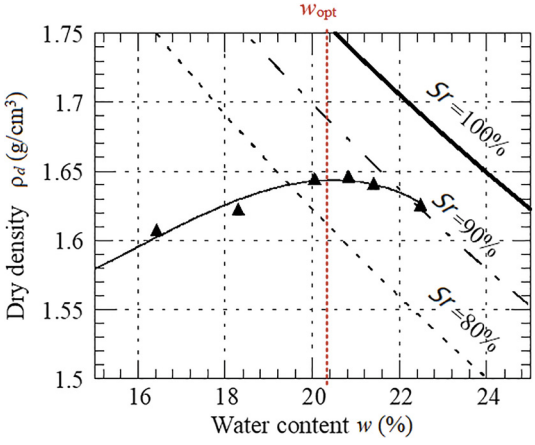

Fig. 13. Compaction curve of Edosaki sand.

set to 92%, which is the construction standard for backfill in precast arch culverts. The backfill was compacted manually in lifts of 50 mm.

In this experiment, almost one week was required for each case from the adjustment of the water content in the Edosaki sand to the commencement of the shaking table tests. Therefore, the ground was covered with bonded textile and plastic sheets to prevent it from drying. After the shaking table tests, the ground water content was measured at 200-mm intervals, and the deviation from the prescribed water content ($w = 20.0\%$) was less than $\pm 1\%$ (Fig. 14). When the model ground was constructed, the ground shear wave velocity was measured by high-sensitivity accelerometers (ARS-10A, produced by Tokyo Sokki Kenkyujo Co., Ltd.) at four points on the left and right sides of the culverts. The shear wave velocity of the ground increased with the depth, and the average velocities were 100, 134, and 209 m/s at the measured points from top to bottom.

4.2 Experimental results

Figure 15 illustrates the change in the culvert inside width. The inside height was calculated from the vertical displacement of the crown with respect to the invert. The inside width was measured at a height of 630 mm from the invert. From the figure, it can be observed that the inner space displacement changed discontinuously when the embankment height was approximately 1.61 m. This is because the construction process extended to the following day at this point and the ground consolidated. When the embankment height was lower than the culvert crown, the displacements of the crown and both shoulders were small, and the behavior presumed in the design was not observed. This is because the experimental model used in this study did not have reduced elastic moduli for the concrete and reinforcing bars in accordance with the experimental scale. Therefore, the culvert model rigidity was relatively large and hardly any displacement was developed

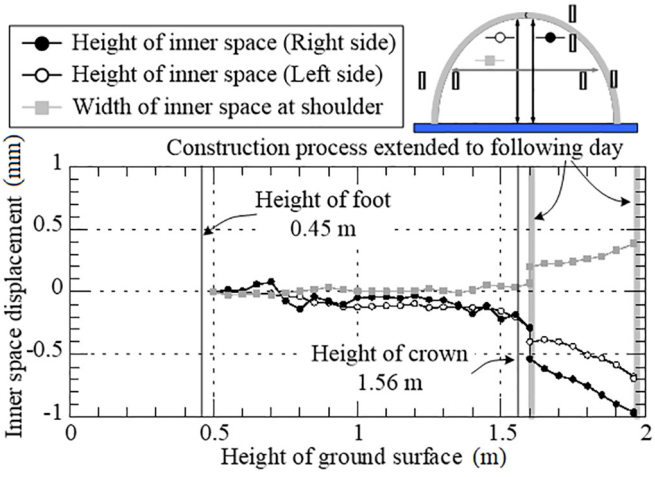

Fig. 15. Change in inside width.

when the height of the embankment was low and the stress acting on the culvert was small. However, when the embankment height was higher than the crown, the crown was displaced inwards and both shoulders were displaced outwards; such a mode is the same as that in the design assumption.

Figure 16 illustrates the rotation angle of the crown hinge across the construction steps. The rotation angle was calculated from the changes in the horizontal displacement inside and outside the culvert surface. The crown hinge was displaced inwards when the embankment height was lower than the crown, while it was displaced outwards when the embankment height was higher than the crown. This behavior indicates a similar tendency to that of the design assumption.

Figure 17 illustrates the coefficient of earth pressure, calculated from the earth pressure acting on the right-hand-side culvert. The earth pressure acting on the culvert was measured by earth pressure gauges directly attached to the culvert. Therefore, the measured earth pressure is the earth pressure in the normal direction to the culvert. When the coefficient of earth pressure was calculated, the horizon-

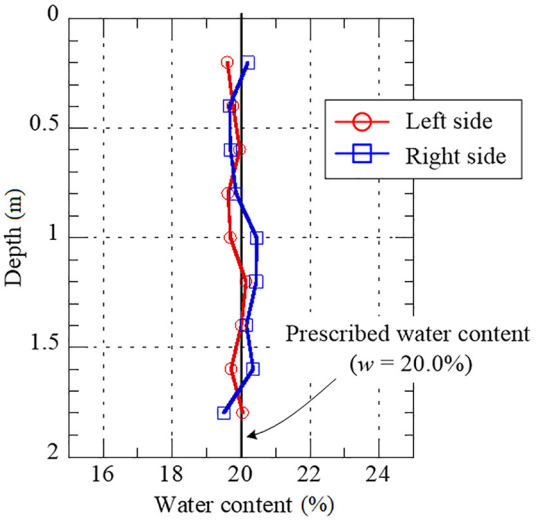

Fig. 14. Water content of model ground after shaking table tests.

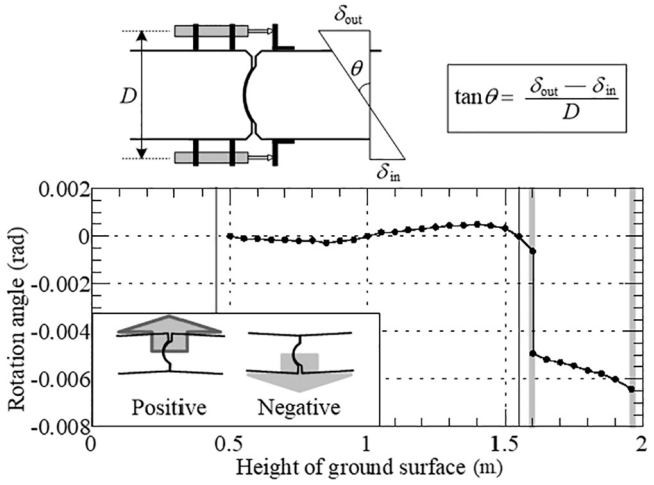

Fig. 16. Change in rotation angle at crown hinge.

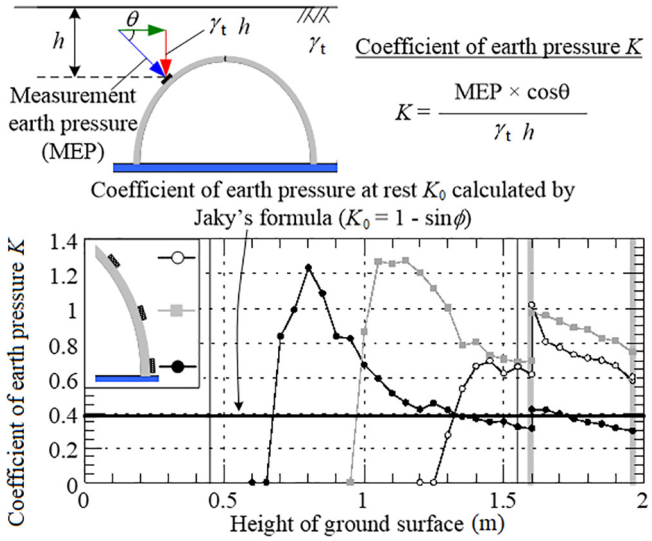

Fig. 17. Change in coefficient of earth pressure acting on right arch element.

tal component was divided by the vertical earth pressure calculated from the soil cover thickness. The coefficient of earth pressure calculated by Jaky's formula (1948) ($K_0 = 1 - \sin\phi = 0.380$) is also indicated in the figure. Although the coefficient of earth pressure K becomes 1 or greater under the influence of compaction, it gradually converges to a steady value. The coefficient of earth pressure K at each position is 0.299, 0.748, and 0.605 from the bottom. As unsaturated Edosaki sand was used for the ground, the ground was self-supported; thus, the earth pressure at rest was expected to be smaller than Jaky's formula. The coefficient of earth pressure at the feet was smaller than the others because the displacement of the feet was so small that the horizontal earth pressure at those points was similar to the earth pressure at rest. However, the horizontal earth pressure was larger than the earth pressure at rest, and acted on the upper parts because the arch was flattened.

Figure 18 illustrates the distribution of earth pressure acting on the culvert during each construction stage. An equal amount of earth pressure acted on both sides of the arch, indicating that the model ground was prepared

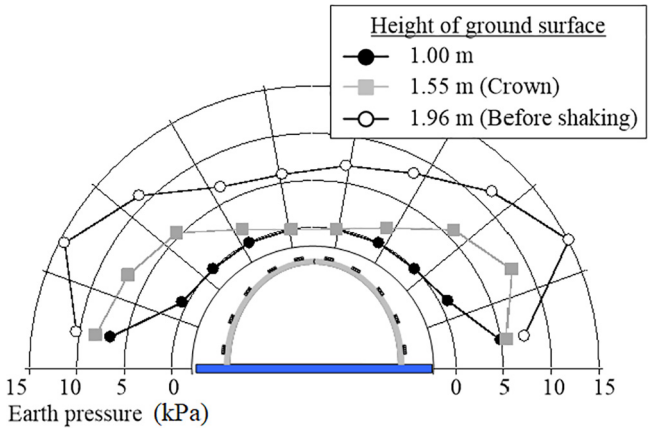

Fig. 18. Distribution of earth pressure acting on arch member.

appropriately. At the end of the construction, the earth pressure around the shoulders was large because the coefficient of earth pressure was large at both shoulders.

Based on the above results, it was determined that the coefficient of earth pressure increased according to the embankment height, although the culvert deformation differed slightly from that predicted in the design.

5 Conclusions

In this study, field measurements and large-scale model tests were conducted on a three-hinge precast arch culvert to analyze the culvert mechanical behavior during the construction process. The following conclusions can be drawn from the results of this study.

[Field measurements]

(1) The inner space displacement of the three-hinge precast arch culvert in the in-situ construction was almost the same as that assumed in the design. The largest horizontal displacement occurred at $h/4$ and $2h/4$, and the horizontal displacement following construction was approximately 13 mm with respect to the culvert width of 9.5 m.

(2) The coefficient of earth pressure around the shoulders ($K = 0.69$) was larger than that around the feet ($K = 0.5$) because of the culvert deformation.

[Model experiments]

(3) When the embankment height was higher than the crown, both the inside width and rotation angle of the crown hinge exhibited the same behavior as that assumed in the design. However, when the embankment height was lower than the crown, the inner displacement differed from that assumed in the design, even though the crown hinge rotation angle was as per the design. This is because the experimental model employed in this study did not use reduced elastic moduli of the concrete and reinforcing bars in accordance with the experimental scale. Therefore, the culvert model rigidity was relatively large and hardly any displacement was developed when the embankment height was low and the stress acting on the culvert was small.

(4) The coefficient of earth pressure at the feet, considered to be relatively close to the coefficient of earth pressure at rest (K_0), was approximately 0.3, while the coefficient of earth pressure around the arch shoulders was more than 0.6. From these results, it was confirmed that the horizontal earth pressure, which was larger than the earth pressure at rest, acted on the arch shoulders.

Acknowledgments

This research was supported by the National Institute for Land and Infrastructure Management, MLIT, Japan

(grant for the research and development of technologies for improving the quality of road policies, no. 24-4, 2012-2015). During the design of the experimental models, members of the Japan Techspan Association provided insightful comments and suggestions.

References

Abuhajar, O., El Naggar, H., & Newson, T. (2015). Static soil culvert interaction the effect of box culvert geometric configurations and soil properties. *Computers and Geotechnics, 69*, 219–235.

Abuhajar, O., El Naggar, H., & Newson, T. (2016). Numerical modeling of soil and surface foundation pressure effects on buried box culvert behavior. *Journal of Geotechnical and Geoenvironmental Engineering, 142*(12), article ID 04016072.

Acharya, R., Han, J., & Parsons, R. L. (2016). Numerical analysis of low-fill box culvert under rigid pavement subjected to static traffic loading. *Journal of Geotechnical and Geoenvironmental Engineering, 16*(5), article ID 04016016.

Adachi, T., Kimura, M., Kishida, K., & Samejima, R. (2001a). Model tests on the earth pressure acting on the precast tunnels. In *Proc. of the regional conf. on geotechnical aspects of underground Construction in soft ground* (pp. 151–156). Shanghai: Tongji University Press.

Adachi, T., Kimura, M., Kishida, K., & Samejima, R. (2001b). Experimental study on stability of the precast concrete tunnel. *International Conference on Modern Tunneling Science and Technology, Swets & Zeilinger* (2, pp. 985–990).

Byrne, P. M., Anderson, D. L., & Jitno, H. (1996). Seismic analysis of large buried culvert structures. Transportation Research Record 1541. Washington, DC: Transportation Research Board (pp. 133–139). Washington, DC: Transportation Research Board.

Debiasi, E., Gajo, A., & Zonta, D. (2013). On the seismic response of shallow-buried rectangular structures. *Tunnelling and Underground Space Technology, 38*, 99–113.

Hushmand, A., Dashti, S., Davis, C., Hushmand, B., Zhang, M., Ghayoomi, M., McCartney, J. S., Lee, Y., & Hu, J. (2016). Seismic performance of underground reservoir structures: Insight from centrifuge modeling on the influence of structure stiffness. *Journal of Geotechnical and Geoenvironmental Engineering, 142*(7), article ID 04016020.

Hutchinson, D. (2004). Application and design of segmental precast arches. *Geotechnical Engineering for Transportation Projects*, 452–459.

Jaky, J. (1948). Pressure in silos. In *Proc. of the 2nd International Conference on Soil Mechanics and Foundation Engineering, Balkema, Rotterdam* (pp. 103–107).

Kagawa, T. (1978). On the similitude in model vibration tests of earth-structures. *Proceedings of Japan Society of Civil Engineers, 275*, 69–77 (in Japanese).

Kim, K., & Yoo, C. H. (2005). Design Loading for Deeply Buried Box Culverts. *Journal of Geotechnical and Geoenvironmental Engineering, 131*(1), 20–27.

Penman, A. D. M., Charles, J. A., Nash, J. K., & Humphreys, J. D. (1975). Performance of culvert under Winscar dam. *Geotechnique, 25* (4), 713–730.

Pimentel, M., Costa, P., Felix, C., & Figueiras, J. (2009). Behavior of reinforced concrete box culverts under high embankments. *Journal of Structural Engineering, 135*(4), 366–375.

Sawamura, Y., Kishida, K., & Kimura, M. (2015). Centrifuge model test and FEM analysis of dynamic interactive behavior between embankments and installed culverts in multiarch culvert embankments. *International Journal of Geomechanics, 15*(3), article ID 04014050.

Sawamura, Y., Ishihara, H., Kishida, K., & Kimura, M. (2016). Experimental study on damage morphology and critical state of three-hinge precast arch culvert through shaking table tests. *Procedia Engineering, Advances in Transportation Geotechnics III, 143*, 522–529.

Segrestin, P., & Brockbank, W. J. (1995). Precast arches as innovative alternate to short span bridges. *Fourth Bridge Engineering Conference, San Francisco, California, USA*.

Vaslestad, J., Johansen, T. H., & Holm, W. (1993). Load reduction on rigid culverts beneath high fills: Long-term behavior. *Transp. Res. Rec.* (1415, pp. 58–68). Washington, D.C.: Transportation Research Board.

Wang, J. N. (1993). Seismic design of tunnels: A state-of-the-art approach Monograph 7. New York: Parsons Brinckerhoff Quade & Douglas.

Wood, J. H., & Jenkins, D. A. (2000). Seismic analysis of buried arch structures. *Proc., 12th World Conf. on Earthquake Engineering, New Zealand Society for Earthquake Engineering, Wellington, New Zealand*.

Wood, T. A., Lawson, W. D., Surles, J. G., Jayawickrama, P. W., & Seo, H. (2016). Improved load rating of reinforced-concrete box culverts using depth-calibrated live-load attenuation. *Journal of Bridge Engineering, 21*(12), article ID 04016095.